MEASUREMENTS ON THE ACOUSTIC ANISOTROPY OF SOFT AND HARD WOOD; EFFECTS ON SOURCE LOCATION

MESSUNGEN ZUR AKUSTISCHEN ANISOTROPIE VON NADEL- UND LAUBHOLZ; EFFEKTE AUF DIE QUELLENORTUNG

MESURE A L'ANISOTROPIE ACOUSTIQUE DE BOIS RESINEUX ET FEUILLUS; INFLUENCE SUR LA LOCALISATION DES SOURCES D'EMISSION ACOUSTIQUE

Thomas Ringger, Lilian Höfflin, Gerhard Dill-Langer, Simon Aicher

SUMMARY

The paper reports on measurements of the acoustic anisotropy of wood, i.e. the dependency of the velocity of ultrasonic bulk waves propagating through wood at different angles between the direction of the wave propagation vector and the principal growth directions. For both, soft wood (represented by spruce) and hard wood (represented by beech), the velocity measurements were conducted by means of transmission method of pulsed ultrasound (US). The main part of the measurements was performed with small cubes of clear wood (for both, spruce and beech), another part with one macroscopic board-like timber specimen (for spruce only). The velocity determination was based on the "time-of-flight" of the US pulses, defined as the time lag between the trigger time of the pulse generator and the on-set time of the transmitted fully recorded signal.

The velocity results showed some characteristic differences for the comparison between spruce and beech with a throughout more pronounced acoustic anisotropy in case of spruce.

Based on the results for spruce, the influence of acoustic anisotropy on the location of "artificial" ultrasound sources has been analysed. The calculation of the source co-ordinates by means of time-of-flight measurements with several spatially distributed transducers forwarded a pronounced improvement of location results, when the empirically obtained acoustic anisotropy was considered.

ZUSAMMENFASSUNG

Der Aufsatz berichtet über Messungen der akustischen Anisotropie des Holzes, d.h. der Abhängigkeit der Körperwellengeschwindigkeit vom Winkel zwischen der Ausbreitungsrichtung und den jeweiligen Anisotropierichtungen. Die Messungen wurden sowohl an Laubholz (repräsentiert durch die Holzart Buche) als auch an Nadelholz (repräsentiert durch die Holzart Fichte) mittels gepulster Ultraschall-Transmission durchgeführt. Der Hauptteil der Messungen wurde mit kleinen würfelförmigen Proben (sowohl für Buche als auch für Fichte) durchgeführt, ein zusätzlicher Teil mit einer makroskopischen Bauholzprobe (nur für Fichte). Die Bestimmung der Ultraschallgeschwindigkeiten basierte auf der Messung der "Pulslaufzeit", definiert als Zeitdifferenz zwischen der Triggerzeit des Pulsgenerators und der Einsatzzeit des transmittierten, vollständig aufgezeichneten Signals.

Die Ergebnisse der Geschwindigkeitsmessungen zeigten einige charakteristische Unterschiede zwischen Fichte und Buche mit einer durchgängig deutlicher ausgeprägten Anisotropie im Falle der Nadelholzart Fichte.

Ausgehend von den Ergebnissen für Fichte wurde der Einfluss der akustischen Anisotropie auf die Lokalisierung von „künstlichen“ Ultraschallquellen analysiert. Die Berechnung der Koordinaten der Quellorte mittels Pulslaufzeit-Messungen an mehreren räumlich verteilten Schallaufnehmern ergab bei Berücksichtigung der akustischen Anisotropie eine deutliche Verbesserung der Lokalisierungsergebnisse.

RESUME

Cet article présente et analyse des mesures d’anisotropie acoustique du bois, i.e. de la dépendance de la vitesse de propagation d’ondes ultrasonores dans le bois vis-à-vis de l’angle entre la direction du vecteur de propagation et les axes principaux de croissance. Les mesures de vitesse ont été effectuées sur un résineux (l’épicéa) et un feuillu (le hêtre) par une méthode basée sur la transmission d’ondes ultrasonores (US). Une partie des analyses a été réalisée sur de petits cubes de bois sans défaut (épicéa et hêtre), et une autre partie sur des spécimens de dimension structurale (épicéa seulement). La détermination de la vitesse est basée sur le temps de propagation de l’onde, défini comme

l'intervalle de temps entre l'impulsion du générateur d'ondes et l'enregistrement du signal transmis par un récepteur.

Les résultats obtenus font apparaître des différences prononcées entre l'épicéa et le hêtre, dont une anisotropie acoustique plus visible dans le cas de l'épicéa.

A partir des résultats obtenus sur l'épicéa, l'influence de l'anisotropie acoustique sur la localisation des sources artificielles d'émission acoustique a été analysée. Le calcul des coordonnées de la source à partir des mesures de temps de propagation jusqu'à des récepteurs spatialement répartis a conduit à une amélioration des résultats de localisation lorsque l'on utilise les valeurs expérimentales d'anisotropie acoustique, plutôt que les valeurs de la littérature.

Nous avons trouvé que la localisation des sources artificielles d'émission acoustique n'est possible que si l'on prend en compte l'anisotropie acoustique.

KEYWORDS: acoustic anisotropy, wood, non-destructive testing, ultrasound, pulse transmission, location of ultrasound sources

1. INTRODUCTION

The location of vibration sources, e.g. earthquake epicentres or acoustic emission sources, by means of relative arrival times of the generated waves at several spatially distributed receivers is an important method for damage characterisation both, in Geophysics and Material Science [6, 7 and 3]. Thereby, the velocity of wave propagation is the decisive parameter for accurate source location results.

While the time-of-flight of pulsed ultrasound (US) in an isotropic medium depends solely on the distance between source and receiver, the transition time in an anisotropic medium depends also on the angles between the pulse wave vector and the directions of the material anisotropy axes. The natural material wood represents growth-bound a pronounced anisotropic material with approximately cylindrical symmetry and three principal directions, being the longitudinal direction (L) parallel to fiber or stem axis, the tangential direction (T) following the curvature of the annual rings and the radial direction (R) perpendicular both, to the tangential and the longitudinal direction.

For the dependency of the wave velocity on the angle between the propagation vector and the growth directions, several studies can be found in literature

[e.g. 1, 2, 11]. Under certain assumptions (pure elastic material law, plane waves, infinite test volume) the acoustic anisotropy can be calculated from the anisotropic stiffness parameters [5, 9]. However, the velocity results due to time-of-flight measurements of ultrasound pulse transmission differ considerably from results due to phase shift method. Moreover, published data vary considerably due to several influencing factors, being e. g. variability within the wood species, boundary conditions of the respective test set-up and pulse shape in the time and frequency domain.

The reported ongoing study aims at the establishment of a reliable empirical data base for the dependency of ultrasound pulse velocity on angle between propagation and principal directions. This is first done for a given set of circumstances, i.e. for two specimen geometries, two wood species and one pulse shape technically bound to the available ultrasound pulse generator. The results shall serve as a basis for an adequate application of the ultrasound source location method for wooden specimens and construction elements.

2. SCOPE OF THE EXPERIMENTAL PROGRAM

The main test series of the reported study comprised time-of-flight measurements on small-sized clear wood specimens with a systematic variation of the angle between propagation direction and principal growth directions. The main test series was conducted with both, beech and spruce wood specimens.

In order to exemplarily apply the results to the location of ultrasound sources, one board-like timber specimen with structural dimensions has been investigated, too. The respective time-of-flight measurements should validate, whether the acoustic anisotropy data from small clear specimens can be transferred to timber in spite of longer flight-paths, a different geometry, uncertainty about the exact angle with respect to the growth directions R and T and the presence of smaller defects.

3. EXPERIMENTAL SET-UP

3.1 Investigated specimens

Following a similar test set-up for measurements on the angle dependent velocity of ultrasonic waves in [5, 9], the clear wood specimens of the main test series were of prismatic (nearly cubic) geometry and small-sized with dimensions (length l × width b × depth h) of 30 mm × 30 mm × 15 mm for both spruce and beech. For the chosen specimen size, in connection with the sawing pattern of the boards further away from pith, the annual ring curvature is negligible. So in an approximation the cylindrical anisotropy of wood reduces to a rhombic orthotropy. The specimens were throughout free of any visible growth defects.

The specimens were cut from solid wood boards in such a manner, that the wider (30 mm × 30 mm) faces of the parallelepipeds were co-planar to one of four selected planes, being the three principal planes of wood (LR, LT and RT) and a plane spanned by the L-vector and a vector within the RT-plane at 45° between R and T principal directions (in the following named L-R/T plane). Figure 1 shows the cylindrical anisotropy of sawn solid wood and a schematic representation of the four acoustically investigated planes.

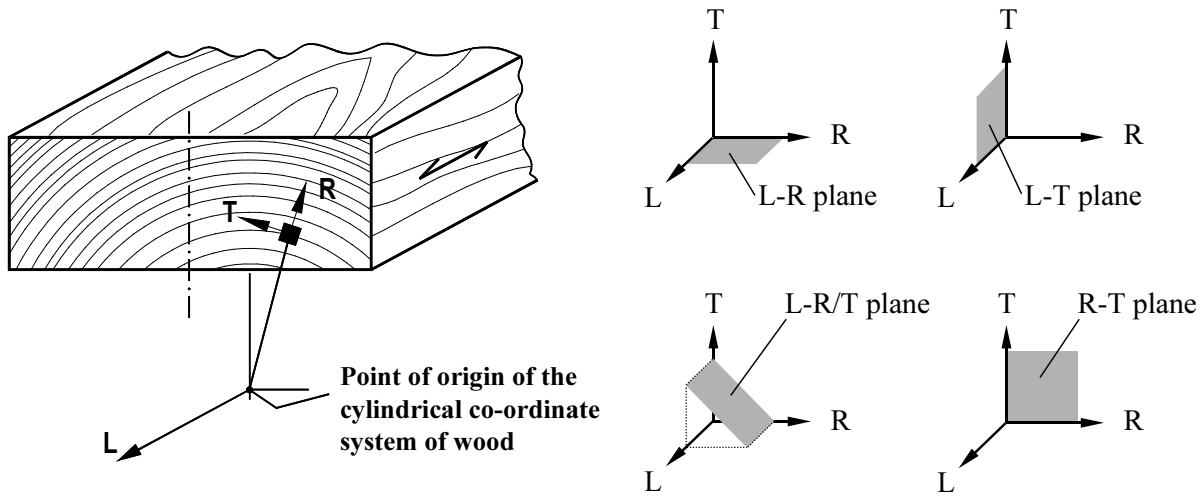

Fig. 1: a) Schematic representation of the cylindrical anisotropy of sawn solid wood b) investigated planes of ultrasound wave propagation

For of each studied plane the angle between the longer (30 mm) edges of the parallelepiped (representing the two orthogonal propagation directions of the pulse transition measurements) and the respective growth directions were varied. The angle is defined as the rotation angle of the material co-ordinate system vs. the two possible directions of the ultrasonic pulse transmission within the regarded planes. Measurements at 0° resp. 90° to the materials axes L, R or T are called on-axis measurements. Pulse transmission tests with specimens including angles unequal to 0° resp. 90° to the material axes are called off-axis measurements. Schematic drawings of the small specimens are shown in the Figures 2a and b. There the vectors $\vec{x}$ and $\vec{y}$ are place holders for the material axes spanning the regarded principal plane. For example in the case of tests on a set of specimens within the RT plane, $\vec{x}$ = R and $\vec{y}$ = T.

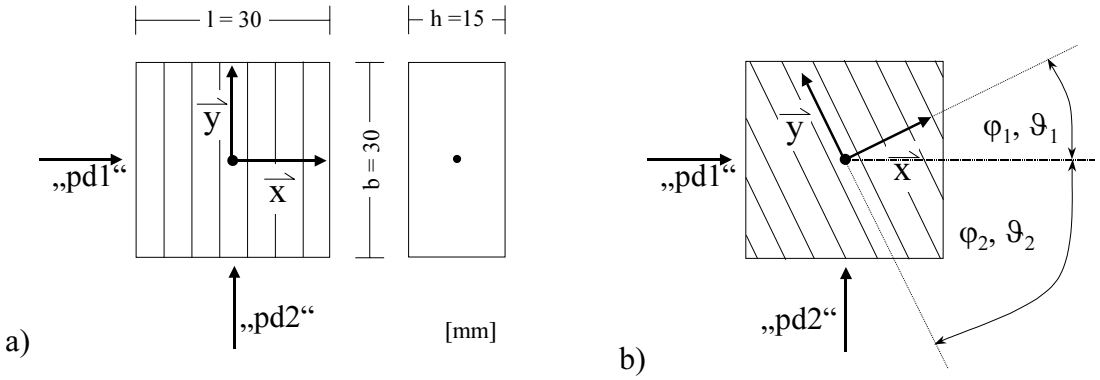

Fig. 2: Sketches of the small clear wood specimens and definitions of on- and off-axis measurements. The ultrasonic pulses are transmitted along the two directions "pd1" and "pd2". $\vec{x}$ and $\vec{y}$ represent the resp. on-axis material co-ordinate directions
a) on-axis and
b) off-axis acoustic measurements

For the planes LR, LT and L-R/T, all including the longitudinal direction L, the off-axis angle φ is defined by the angle between the L direction and the chosen propagation direction ("pd1" or "pd2"). For the measurements on specimens in the RT plane, the off-axis angle ϑ is defined as the angle between the respectively chosen pulse transmission direction ("pd1" resp. "pd2") and the radial (R) direction. The definitions for φ and ϑ are depicted in Figures 3a and 3b.

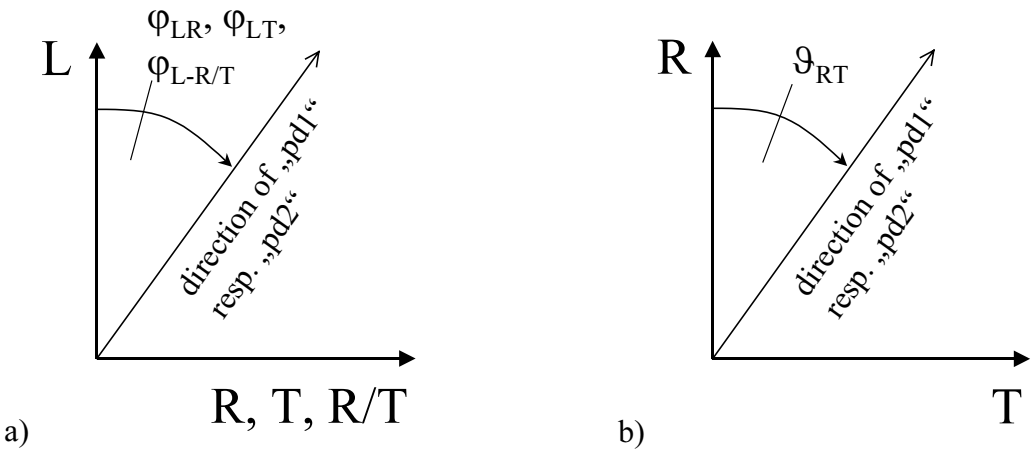

Fig. 3: a, b) Definitions of the regarded off-axis angles
a) φ for the planes including the L direction
b) ϑ within the RT plane

Table 1 specifies the test program with the small clear specimens conducted so far.

The exemplary investigated board-like spruce specimen had the dimensions (length l × width b × depth h) of 500 mm × 120 mm × 25 mm with length l parallel to fibre direction (see Fig. 4). Within the cross-section b × h, contrary to the small clear specimens, the annual ring curvature was non-negligible, resulting in angles of 0 to about 80° between depth direction h and radial growth direction. The normal density of the specimen was $\rho_{12} = 428$ kg/m^3 , the mean year ring width 2.1 mm and the moisture content 8%. The specimen had been selected carefully in order to incorporate as few and as small visible defects as possible. However, compared to the small clear specimens, some defects such as minor small knots or fibre deviations were accepted.

Table 1: Test program for small clear specimens; given are the number of measurements and specimens per investigated plane, angle and species

regarded plane, angle and species		number of measurements per angle										total number of specimens
L-R	angle	0°	15°	30°	45°	60°	75°	90°				
	beech	3	3	3	6	3	3	3				12
	spruce	2	2	2	4	2	2	2				8
L-T	angle	0°	15°	30°	45°	60°	75°	90°				
	beech	3	3	3	6	3	3	3				12
	spruce	2	2	2	4	2	2	2				8
L-R/T	angle	0°	15°	30°	45°	60°	75°	90°				
	beech	1	1	1	2	1	1	1				4
	spruce	1	1	1	2	1	1	1				4
R-T	angle	0°	22.5°	45°	67.5°	90°						
	beech	2	2	4	2	2						6
R-T	angle	0°	15°	22.5°	30°	45°	60°	67.5°	70°	80°	90°	
	spruce	6	1	5	1	6	1	3	1	1	3	23
total number of small clear **beech** specimens:												34
total number of small clear **spruce** specimens:												43

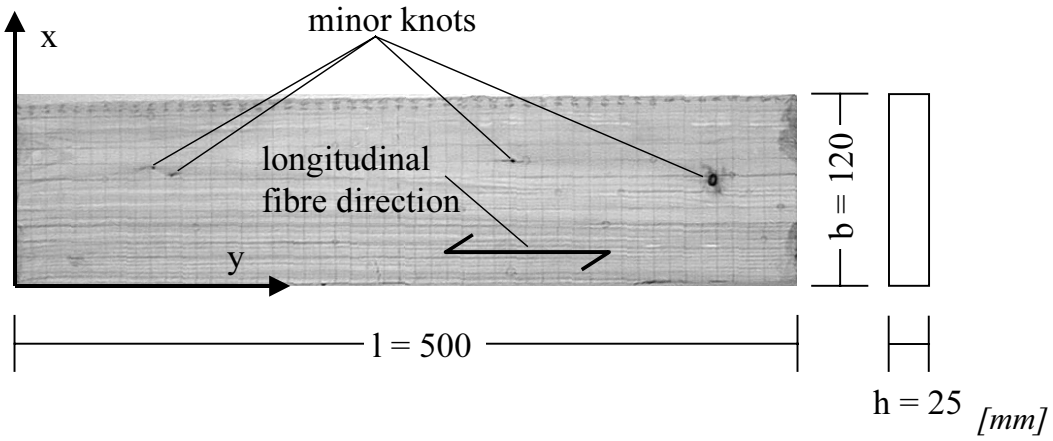

Fig. 4: View and dimensions of the board-shaped specimen's surface

3.2 Realisation of the measurements

The determination of the acoustic properties of the small clear specimens of spruce and beech was throughout performed by means of a pair of piezoelectric (US) transducers. For each single specimen an ultrasonic pulse synthesised by a generator unit was applied to the centre of one of the specimen's surfaces (15 mm × 30 mm) by the piezoelectric transmitter. The receiver was positioned at the centre of the opposite surface, leading to a length of the assumed straight pulse path of 30 mm. In all test series the transmitter and the receiver were fixed to the surface by a hot melt adhesive. Thus, the adhesive served as a coupling agent, too. Figure 5 shows a schematic view of the experimental set-up for the small clear specimens. For each specimen three repetitive measurements (3 US pulses) per direction of pulse transmission were performed.

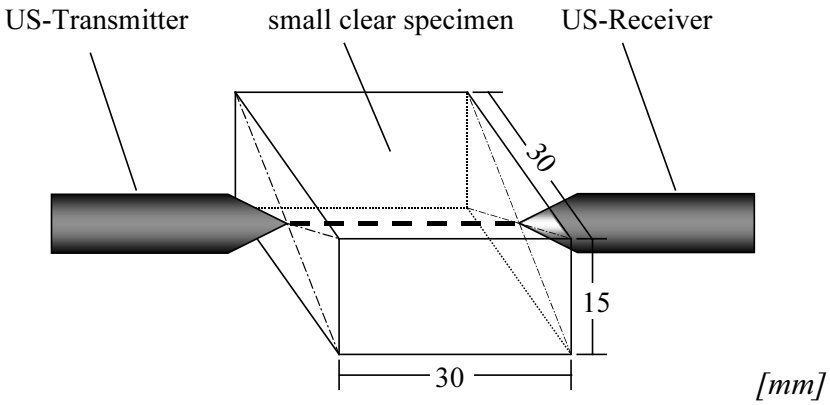

Fig. 5: Scheme of the experimental set-up of the measurements on the small cubic specimens.

The measurements on the board-shaped specimen were performed as following. Ultrasonic pulses were applied to one of the wide faces of the specimen at deliberately chosen "source points" denoted by co-ordinates (x^s, y^s). The ultrasound waves propagating through the specimen were then recorded by six spatially distributed ultrasonic receivers at fixed positions as shown in Fig. 6. The propagation of the pulse waves to each of the receivers (A - F) was assumed to follow a straight path between the source and the respective receiver. For each “source point” and each receiver, the distance and the respective angle enclosed with the longitudinal fibre direction was recorded.

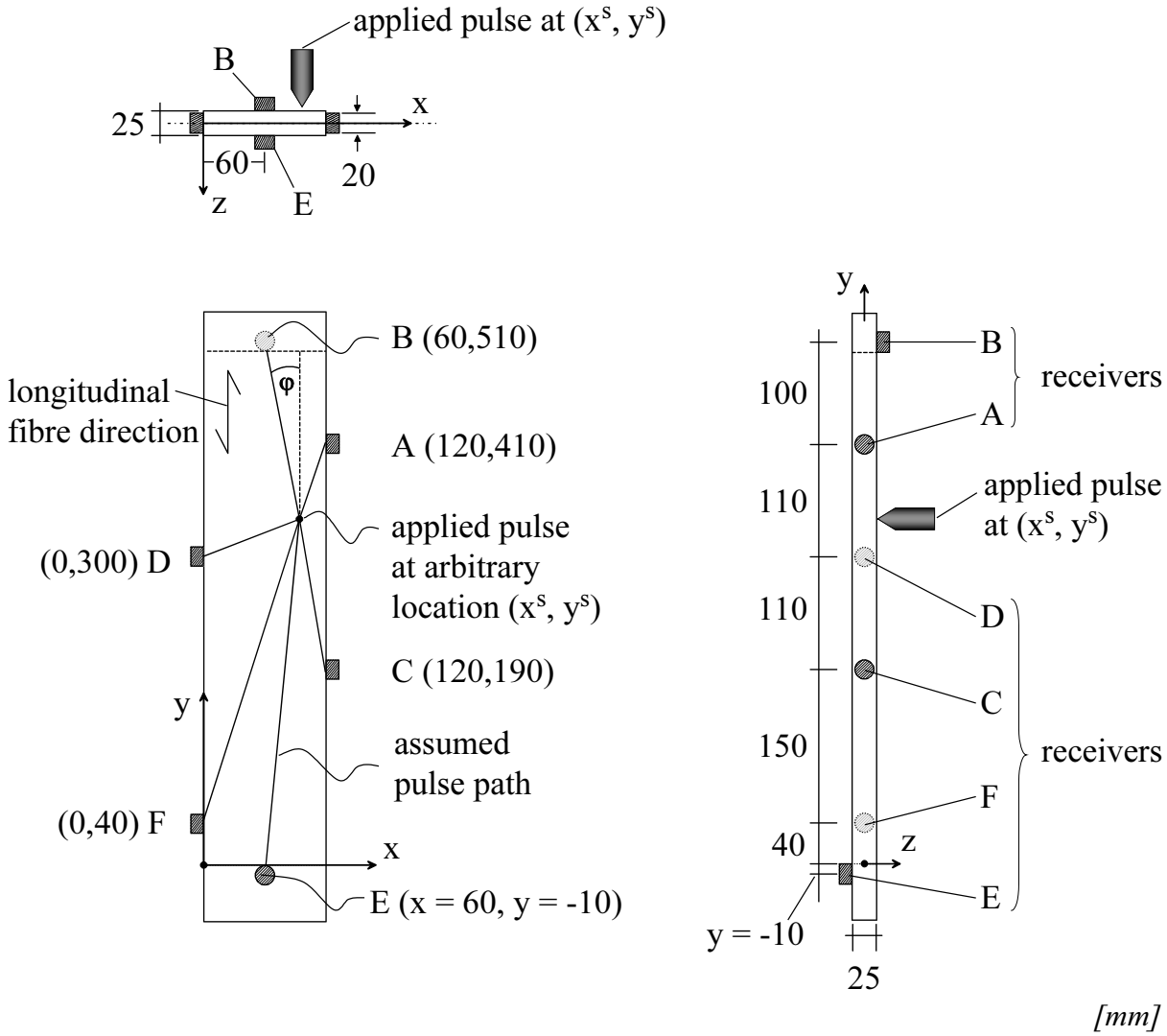

Fig. 6: Test set-up and dimensions of the tests with the board-shaped spruce specimen

3.3 NDT Equipment

The employed generator unit (USG 20; Geotron Electronics), originally optimised for NDT measurements on concrete, produces high voltage pulses. The main frequencies of the pulses are between 20 kHz and 350 kHz and the duration of a single pulse is less than 1 ms. Simultaneously with applying a synthesised pulse, the apparatus gives out a trigger impulse, defining the zero point on a time axis.

The employed ultrasonic transducers (= transmitter and receivers) comprised two different types of piezoelectric converters, both types showing a multi-frequency characteristic with a main sensitivity between 20 and 150 kHz.

i) The measurements on the small clear specimens were performed with an ultrasonic transmitter (UPG-D) and a receiver (UPE-D), both by Geotron Electronics. The diameter of the coupling surface of the transducers is 3 mm.

ii) For the board-shaped specimen, the mentioned ultrasonic transmitter UPG-D was used. Differently now, six receivers of type VS150-M (vallen systeme) were employed. The size of the coupling surface of the receivers is 20 mm in diameter.

The received ultrasonic pulses were amplified by a broadband amplifier (AM 502; Tektronix) with a maximum amplification factor of 100 dB. The complete signals were recorded with a PC based transient recorder with 12 bit amplitude and 20 MHz time resolution.

3.3 Characterisation of signal-parameters

The ultrasonic pulses were detected as chronologically oscillating voltages with limited duration, being typical for events with burst-like disposal of energy.

In the context of this paper, the recorded signals were evaluated exclusively for “time-of-flight” (TOF), defined as the time lag between the externally given zero time point t_0 and the on-set (begin) of the recorded signal. The definition of the signal on-set used for the signal evaluation in the context of this paper is discussed in detail in [2, 3]. Figure 7a shows a typical full signal recorded in the performed tests; the derived signal parameter TOF is depicted in Fig. 7b. Trivial, but for sake of “clarity”, the velocity of the ultrasonic pulse was determined as $v = s / TOF$ where s is the distance between transmitter and receiver.

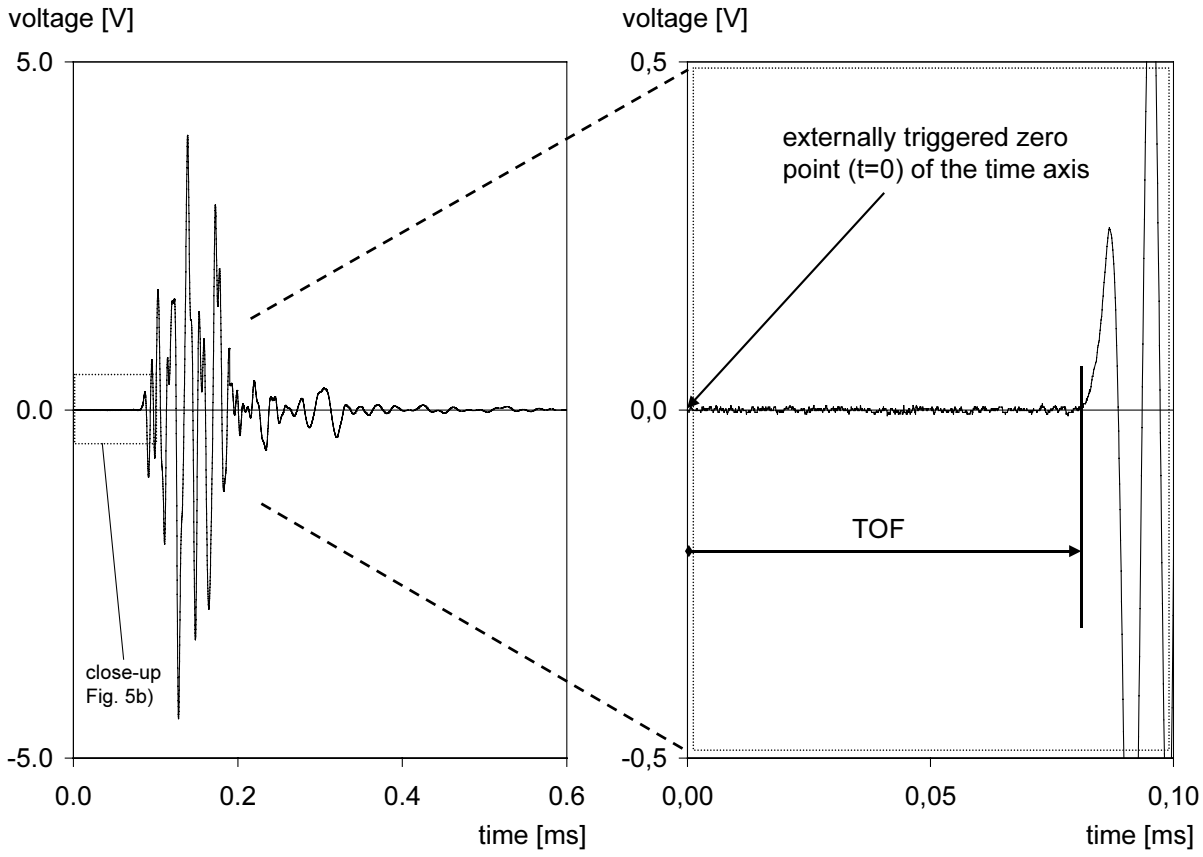

Fig. 7: Graph of a typical signal
a) full signal b) close-up with definition of signal parameter TOF

4 RESULTS OF WAVE VELOCITIES FROM SMALL CLEAR SPECIMENS

The results of ultrasonic pulse velocity measurements for planes including the longitudinal direction (LR, LT and L-R/T) are depicted in Figures 8a – c. In detail, Figure 8a shows the dependency of US velocity on off-axis angle φ_{LR} within the principle LR-plane spanned by the longitudinal (L) and radial (R) directions. Analogously, Figure 8b gives the relationship of velocity vs. off-axis angle $v(\varphi_{LT})$ in the LT-plane and Figure 8c contains the results for the L-R/T-plane. In each of the Figures 8a to 8c, the individual results for spruce are depicted as open symbols and filled symbols are used for beech. The plotted lines

connect the mean values or single data points in the case when only one result per angle exists.

From the Figures 8a-c the following observations can be stated:

- The acoustic anisotropy in the LR- and LT-planes is quite similar, for both, spruce and beech. The difference between the maximum velocity values in L-direction and the minimum values in directions perpendicular to fiber direction is about 4500 m/s for spruce and about 3500 m/s for beech, i.e. the acoustic anisotropy in the LR-and LT-planes is considerably more expressed for the softwood spruce.
- In the L-R/T-plane a somewhat reduced acoustic anisotropy can be observed as compared to the results obtained for the principal LR- or LT-planes. The difference between maximum and minimum velocity values is about 4100 m/s for spruce and 3100 m/s for beech. In the velocity vs. angle curves it is obvious that for small angles to fibre direction (about $\varphi = 15°$) the span between spruce and beech is considerably smaller in comparison with the LR- and LT-planes.

The results of measurements in the RT-plane of spruce and beech have already been reported in detail in [2, 3]; here only a short summary is given. Figure 9 shows the results for $v(\vartheta_{RT})$ within the RT-plane perpendicular to fiber direction. The fitted approximation curves are polynomials of 6^{th} degree.

The difference between the maximum and the minimum values of the ultrasonic wave velocity was about 500 m/s for both wood species and the maximum value was in both cases observed for $\vartheta_{RT} = 0$, i.e. for the R-direction.

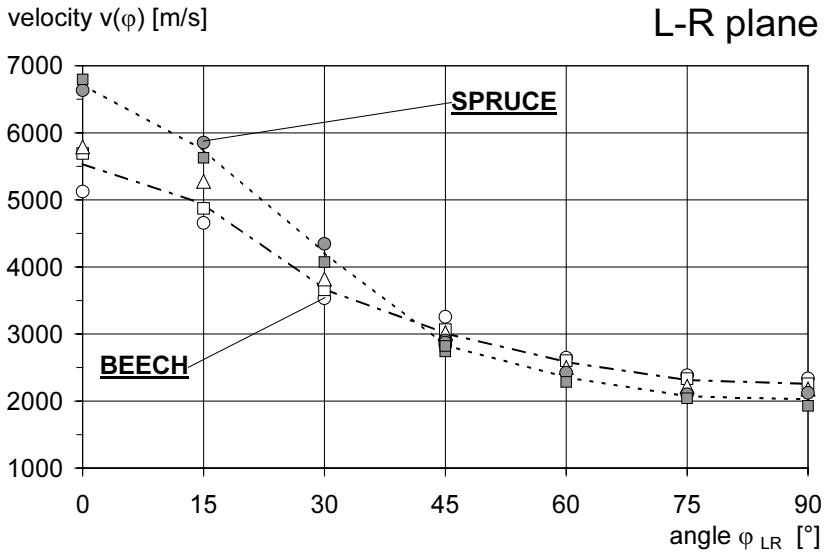

a)

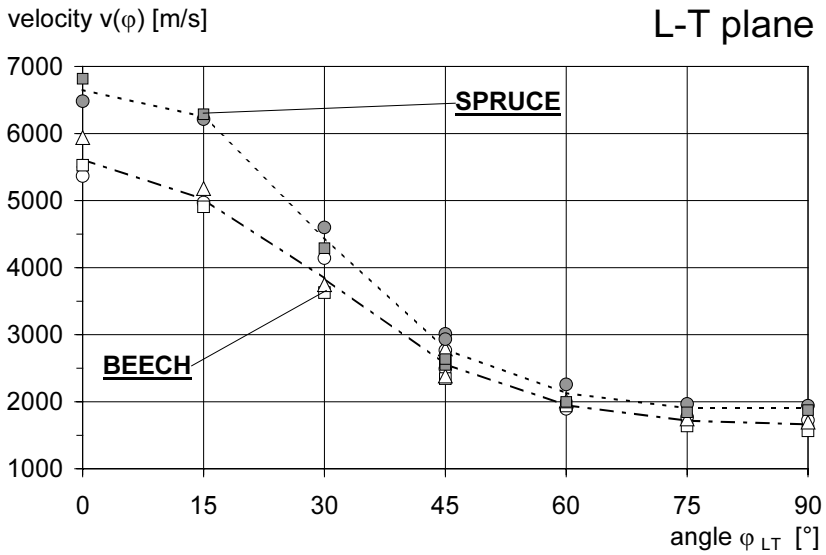

b)

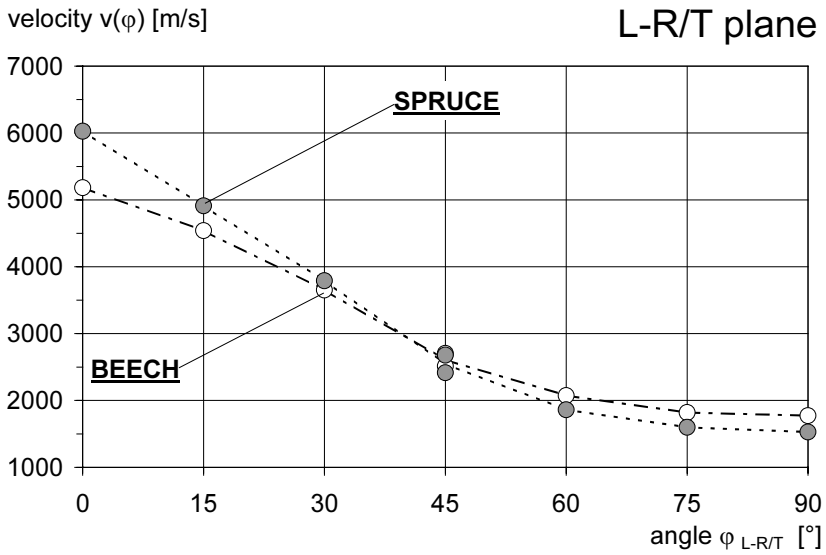

c)

Fig. 8: Ultrasonic wave velocities of wood from small clear specimens
a) L-R-plane b) L-T-plane c) L-R/T-plane

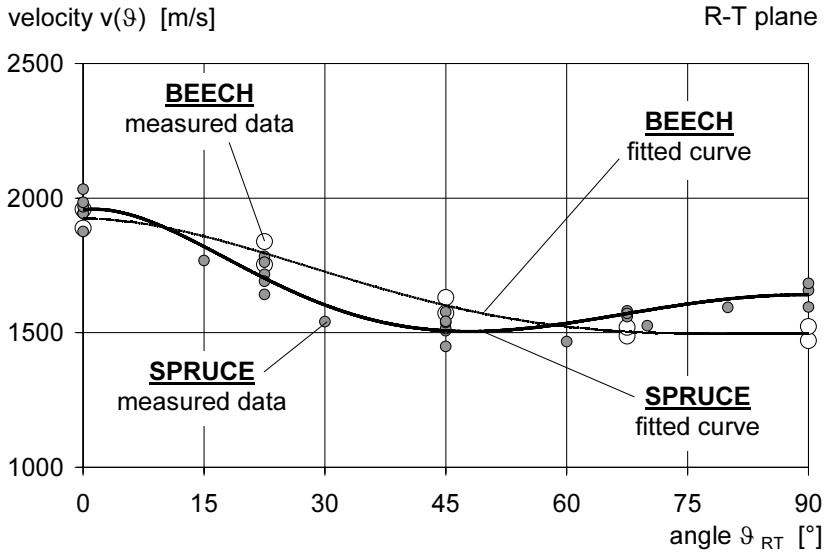

Fig. 9: Ultrasonic wave velocities from small clear specimens in the R-T-plane

While the velocity of ultrasonic waves in beech is monotonically decreasing with a rotation of the transmission direction from the radial to the tangential axis, the results for spruce behave different: At an off-axis angle of about $\vartheta_{RT} = 45°$ a local minimum of 1500 m/s occurs with subsequently increasing velocities towards the tangential direction. The velocity span between radial direction (about 2000 m/s) and the tangential direction (about 1700 m/s) is about 300 m/s, being roundly 200 m/s smaller than the absolute span between R- and intermediate (45°-) direction. In [2, 3] the reason for the local velocity minimum value of soft wood at an angle of about 45° between R- and T-axis, being the shear coupling effect in combination with a very low shear modulus of soft wood, is discussed in detail.

5 WAVE VELOCITIES FROM LARGE SPRUCE TIMBER SPECIMEN

As lined out in chap. 3, for each deliberately chosen "source point" the applied US pulse was received by 6 spatially distributed receivers. This, in general delivers 6 different wave paths, each with different length and angle to fiber direction and hence 6 different velocity values are obtained. The results for the angle dependent wave velocities evaluated from 34 "source points" (i.e. $34 \times 6 = 204$ wave velocities) are shown in Figure 10a all together with a fitted approximation curve (6^{th} order polynomial). For purpose of easier comparison,

the L-R/T-curve from the small clear specimens (as given in Fig. 8c) is additionally plotted in Fig. 10a.

In order to enable an easier visual assessment of the influence of the different specimens' scales and geometries, Fig. 10b repeats the results for the specimen as given in Figs. 8a-c. The synopsis of Figs. 10a and b reveals that the on/off-axis wave velocity of the small clear specimens in the L-R/T-plane agrees best with the results for the large board-shaped specimen. This can be understood qualitatively, as the wave propagation in the board-shaped specimen is somewhere between the L-R- and L-T-plane.

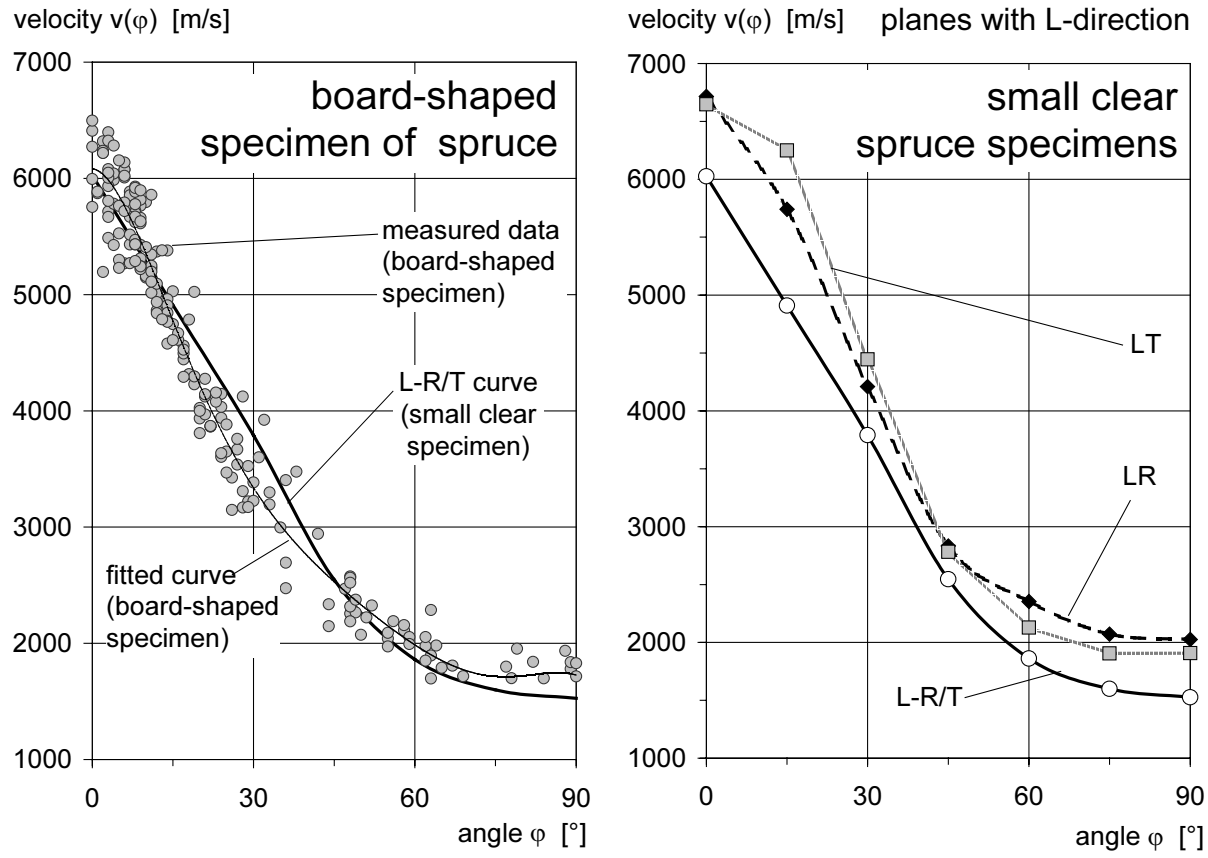

Fig. 10: Angle dependency of the ultrasonic pulse velocity
a) obtained from the board-shaped specimen
b) obtained from the small clear specimens

6 DETAILS TO THE LOCATING METHOD

The algorithm to calculate the co-ordinates of US pulse sources is based upon a minimisation function, where calculated runtimes t^{calc} for assumed source locations (x^{test}, y^{test}) are compared with runtimes t^{emp} estimated by evaluating the signals recorded during the experiment. The minimisation of the Residual function R^2, given by Eq. (1) describing the summation of squared and weighted differences between the calculated and the measured (relative) runtimes yields the estimated source location (x^{source}, y^{source}):

$$R^2\left(x^{test}, y^{test}\right) = \sum_n \left(\frac{\left(t_n^{emp} - t_0^{emp}\right) - \left(t_n^{calc}\left(x^{test}, y^{test}\right) - t_0^{calc}\right)}{t_n^{emp}} \right)^2 \tag{1}$$

$$\text{Min}(R^2) \Rightarrow (x^{source}, y^{source}) \tag{2}$$

Time t_0^{calc} represents the shortest of the N calculated runtimes, where N gives the number of the used receivers; t_0^{emp} is the shortest of the N measured runtimes. Time t_n^{calc} is calculated from the measured data and the geometry of the experimental set-up:

$$t_n^{calc}\left(x^{test}, y^{test}\right) = \frac{\ell_n}{v(\varphi)} \tag{3}$$

where

n = index of the investigated receiver at the surface of the specimen,

$$\ell_n = \sqrt{\left(x_n^{receiver} - x^{test}\right)^2 + \left(y_n^{receiver} - y^{test}\right)^2}$$

and $v(\varphi)$ = anisotropic US pulse velocity given in Fig. 10a for the board-shaped specimen.

6.1 Effect of acoustic anisotropy on source location

From qualitative considerations it is obvious that different assumptions on the acoustic anisotropy of wood will lead to pronouncedly different results of pulse source location. In a thorough analysis of the topic, to be analysed in a separate paper, several assumptions should be evaluated and compared, including the wave velocity results of small clear specimens (LR, LT and L-R/T), the analytical v(φ)-curve due to plane-wave approximation [5, 9] and empirical re-

sults from different literature sources. In the frame of the reported ongoing study, two simple assumptions have been tested, being the extreme cases of isotropic behaviour and anisotropic behaviour due to empirical velocity measurements at the exemplary regarded board-like timber specimen.

In order to quantify the dimension of the locating error induced by the use of isotropic pulse velocities, the following numerical values were employed:

A1: v_{A1} = const. = 6089 m/s = maximum of measured velocities

A2: v_{A2} = const. = 1640 m/s = minimum of measured velocities

A3: v_{A3} = const. = 3865 m/s = mean value of v_{A1} and v_{A2}

The comparison of the predetermined co-ordinates of the US pulse sources with the calculated co-ordinates enables the quantification of the locating error, here defined as the difference between the applied and the estimated US pulse source co-ordinates. Table 2 specifies the mean values and the standard deviations of the location error which are given separately for the direction perpendicular (x co-ordinate) and parallel (y co-ordinate) to fibre direction.

It can be seen that the best isotropic assumption for the pulse velocity is given by the maximum measured velocity (6100 m/s). This results in mean differences between estimated and applied co-ordinates of $\Delta x = 32$ mm in directions perpendicular and $\Delta y = 29$ mm parallel to the longitudinal direction, respectively.

In a first preliminary evaluation of the effect of correct / incorrect anisotropic velocities on the location error, the velocity results of the board-shaped timber specimen as given in Fig. 10a is employed. Table 3 specifies the achieved locating “accuracy”; for comparison the errors of the best isotropic solution (v_{A1}) are given, too. As anticipated qualitatively, it is revealed that the consideration of the empirically determined anisotropy leads to a highly increased location accuracy. The expressed improvement of the location accuracy for all individual artificial pulse sources is revealed graphically in Figs. 11a and 11b which shows the location results for the “best” isotropic velocity and the anisotropic pulse velocity.

Table 2: mean values and standard deviations for the differences between applied and numerically estimated NDT source co-ordinates, neglecting acoustic anisotropy properties

Differences between applied and estimated US pulse source co-ordinates a) perpendicular to the longitudinal fibre direction (x-axis of the specimen)			
assumed v [m/s]:	v_{A1} = 6089	v_{A2} = 1640	v_{A3} = 3865
mean value Δx [mm]:	32	48	36
standard deviation [mm]:	17	26	20
b) parallel to the longitudinal fibre direction (y-axis of the specimen)			
assumed v [m/s]:	v_{A1} = 6089	v_{A2} = 1640	v_{A3} = 3865
mean value Δy [mm]:	29	41	31
standard deviation [mm]:	23	27	20

Table 3: Differences between applied and numerically estimated US pulse source co-ordinates; mean values and standard deviations of the isotropic and the anisotropic case

Differences between applied and estimated co-ordinates of US pulse sources a) perpendicular to the longitudinal fibre direction (x-axis of the specimen)		
assumed v [m/s]:	value of best isotropic fit	fitted curve to the measured anisotropic velocity data
mean value Δx [mm]:	32	4
standard deviation [mm]:	17	3
b) parallel to the longitudinal fibre direction (y-axis of the specimen)		
assumed v [m/s]:	value of best isotropic fit	fitted curve to the measured anisotropic velocity data
mean value Δy [mm]:	29	6
standard deviation [mm]:	23	4

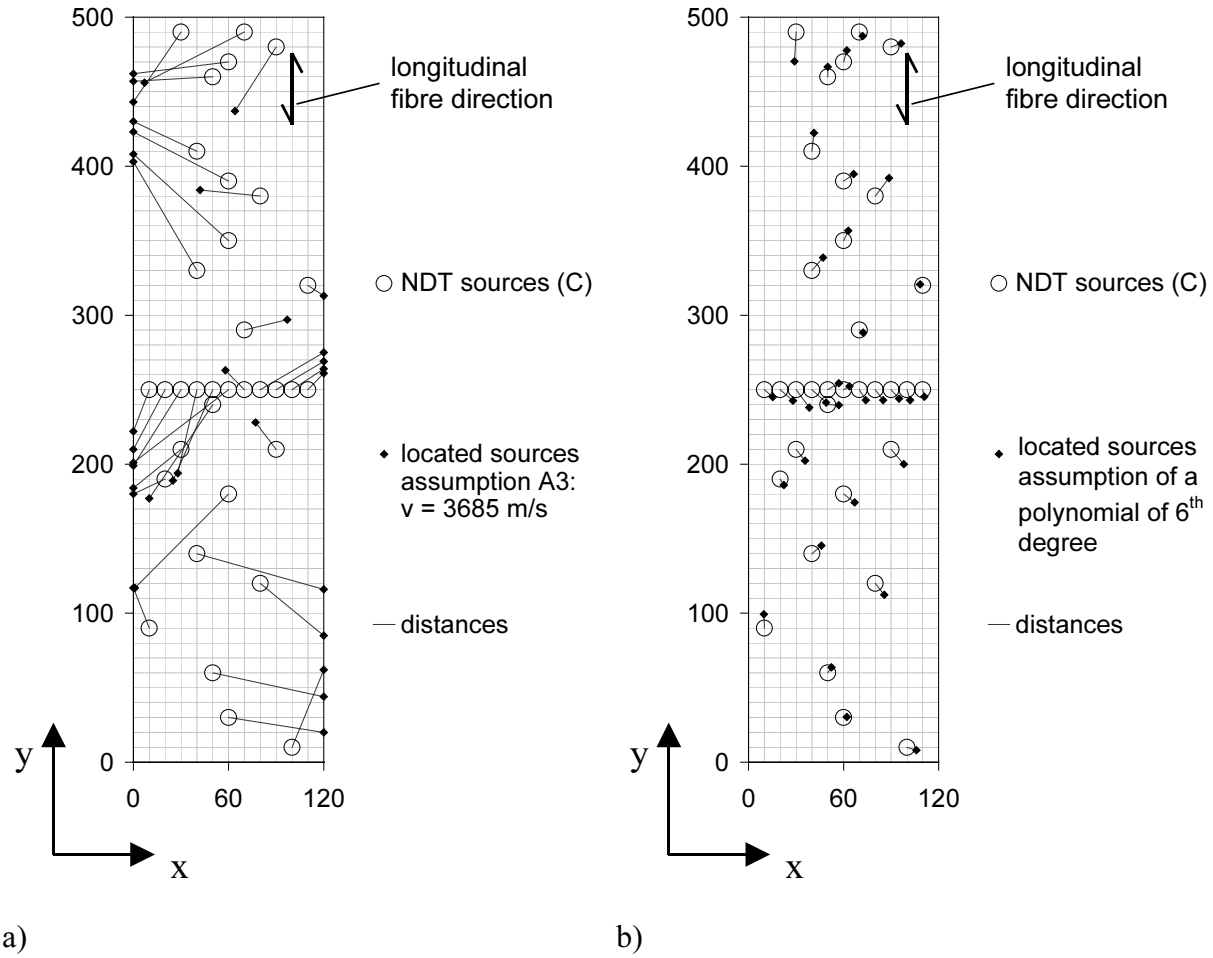

Fig. 11: Applied and estimated co-ordinates of ultrasonic pulse sources on a board-shaped specimen of spruce resulting from
a) isotropic assumption v = const. for the ultrasonic wave velocity
b) best fit curve to the results of the measured anisotropic velocity

7. CONCLUSIONS

The presented preliminary results of the ongoing study on the impact of acoustic anisotropy on location of ultrasound pulse sources can be summarised as following

- The US pulse transmission method on small clear specimens is an apt method in order to establish a database for acoustic anisotropy. By the reported results the anticipated differences between hard wood (beech) and soft wood (spruce) species could be reproduced.
- The velocity measurements on an exemplary board-like timber specimen (made of spruce) were in good accordance with the results for small clear spruce specimens in the L-R/T-plane, i. e. an intermediate

plane spanned by the longitudinal fibre direction and a perpendicular direction within the RT-plane at an angle of 45° to the principal axes.

- The numerical location procedure of ultrasound pulse sources applied to the surface of the exemplary studied timber specimen yielded reasonably low error values, when the empirically calibrated approximation function based on velocity measurements was applied.

Of course, the preliminary results with respect to range of location error cannot be generalised on the basis of only one exemplary timber specimen being used for both, velocity calibration and test of location accuracy. Therefore the study will be prolonged with more specimens taking into account also the variability of the natural material wood by different defect structures and different raw densities.

ACKNOWLEDGEMENTS

The continuous good co-operation between Wood and Timber Construction Department of Otto-Graf-Institute and Laboratoire de Rhéologie du Bois de Bordeaux (LRBB) is gratefully acknowledged. Special thanks are indebted to the director of LRBB, Dr. Patrick Castera, in this context, for his repeated yearly favor of French translation of our OGI-paper abstracts.

The financial support of German Science Community (DFG) via grant to Sonderforschungsbereich 381 “Characterisation of damage evolution in composite materials using non-destructive test methods” and hereby to sub-project A8 “Damage and NDT of the natural fibre composite material wood” is gratefully acknowledged.

REFERENCES

[1] BUCUR, V.: *Acoustics of wood.* Boca Raton, New York, London, Tokyo, 1995, p. 121

[2] HÖFFLIN, L.; AICHER, S.: *Wave velocities in the radial-tangential growth plane of spruce and beech.* COST, Proceedings of the International Conference on Wood and Wood Fiber Composites, Stuttgart, 2000

[3] AICHER, S.; HÖFFLIN, L., DILL-LANGER, G.: *Damage evolution and acoustic emission of wood at tension perpendicular to fibre.* Holz als Roh- und Werkstoff 59, p. 104-116, Springer Verlag, 2001

[4] DILL-LANGER, G.; RINGGER, T.; HÖFFLIN, L.; AICHER, S.: *Location of Acoustic Emission Sources in Timber Loaded Parallel to Grain.* Proc. 13th International Symposium on NDT of Wood, Berkley, California, 2002

[5] BUCUR, V.; ARCHER, R. R.: *Elastic constants for wood by an ultrasonic method.* Wood Science and Technology 18, p. 255-265, Springer Verlag, 1984

[6] GEIGER, L.: *Herdbestimmung bei Erdbeben aus den Ankunftszeiten.* Nachrichten von der Königlichen Gesellschaft der Wissenschaften zu Göttingen 4, p. 331-349, 1910

[7] SALAMON, M. D. G.; WIEBOLS, G. A.: *Digital location of seismic events by an underground network of seismometers using the arrival time of compression waves.* Rock Mechanics 6, p. 141-166, Springer Verlag, 1974

[8] BARON, J. A.; YING, S. P.: *Acoustic emission source location.* Acoustic Emission Testing (Non-destructive testing Handbook, 2nd ed., Vol. 5), p. 145-154, edt. by Miller, R. K. and McIntire, P., American Society for Non-destructive Testing, 1987

[9] BUCUR, V.: *Wood characterisation through ultrasonic waves.* NATO ASI series / E, No. 126, p 323 - 333, 1987

[10] AICHER, S.; DILL-LANGER, G.: *Fracture location by NDT in glulam loaded in tension perpendicular to the grain.* Proc. 11th Int. Symp. Non-destructive Testing of wood, p. 43-54, Forest Products Soc., Madison, USA, 1999

[11] BEAL, F. C.: *Overview of the use of ultrasonic technologies in research on wood properties.* Wood Science and Technology, 36, p. 197-212, Springer Verlag, 2002